

Experimental and Computational Analysis of Microbial Inactivation in a Solid by Ohmic Heating Using Pulsed Electric Fields

M. Á. Ariza-Gracia^{a,b}, M. P. Cabello^a, G. Cebrián^c, B. Calvo^{a,d}, I. Álvarez^c

^aAragón Institute for Engineering Research (ISA), University of Zaragoza, Zaragoza, Spain.

^bARTORG Center for Biomedical Engineering Research, University of Bern, Switzerland.

^cDepartamento de Producción Animal y Ciencia de los Alimentos. Tecnología de los Alimentos. Facultad de Veterinaria. Instituto Agroalimentario de Aragón (IA2). Universidad de Zaragoza, Zaragoza, Spain.

^dCentro de Investigación Biomédica en Red en Bioingeniería, Biomateriales y Nanomedicina (CIBER-BBN), Spain.

Abstract

Pulsed electric field technology (PEF) has traditionally been used as a technique to inactivate microorganisms in liquid foods at temperatures below those used in heat treatments; however, application of high-intensity PEF ($E > 1$ kV/cm) at high frequencies (> 10 Hz) can allow rapid and volumetric solid food electrical heating in order to replace traditional convection/conduction heating that progresses from the heating medium to the inside of the product. This investigation is the first one to evaluate the inactivation of *Salmonella* Typhimurium 878 in a solid product (cylinder of technical agar used as reference solid) by applying PEF treatments (2.5 and 3.75 kV/cm, and up to 9,000 microseconds) at 50 Hz. The evolution of temperature in different locations of the agar cylinder was measured by observing the variability of heating rates depending on location and PEF intensity. Microbial inactivation was determined and compared with isothermal heat treatments that predicted similar inactivation values, but did not detect additional inactivation. Computational analysis enabled us to predict temperature and microbial inactivation for any spatial and temporal distribution of the cylinder agar by detecting the coldest point in the transition zone between the high-voltage electrode, the agar, and the plastic container of the treatment chamber. In order to evaluate the variability of the temperature, computational predictions were done each 0.5-mm. The difference between the coldest and the hottest point (e.g. at the center of the cylinder) resulted in around 10 °C and 10 seconds variation in temperature and processing time, respectively. In any case, it was possible to obtain 5- \log_{10} -reductions after 60 seconds of PEF treatments when using 2.5 kV/cm and 50% reduction for 3.75 kV/cm. These results suggested the potential of PEF technology as a rapid heating system based on ohmic heating for microbial inactivation in solid food products.

1. Introduction

Pulsed electric fields (PEF) technology has been extensively investigated, and is currently being applied by the food industry as an alternative to the thermal pasteurization of liquid products, mainly fruit juices. Thanks to the electroporabilizing effect of PEF, vegetative cells of pathogenic and spoilage microorganisms can be inactivated using lower temperatures than those applied in thermal treatments, thereby permitting the food industry to maintain fresh-like characteristics of foods (Buckow, Ng, & Toepfl, 2013). PEF treatment applies electric fields of high intensity (>0.1 kV/cm) and short duration (from milliseconds to microseconds) to a product placed between two electrodes with only a minimal increase in product temperature, or at least, with an aim to minimize thermal effects (Barbosa-Canovas, Fernandez-Molina, & Swanson, 2001). However the application of a voltage between two electrodes separated by a certain distance (electric field) within which the product to be treated by PEF is placed leads to the passage of an electrical current that induces ohmic heating of the product by Joule effect. This heating effect (W) is defined according to the following equation:

$$W = \int_0^{\omega} \sigma \mathbf{E}^2 dt \quad (1)$$

where σ is the electrical conductivity of the treated medium or product (S/m), \mathbf{E} is the electric field strength (V/m); and dt is the time (s) during which the field strength is applied (Sastry & Li, 1996).

This indicates that any increment in these parameters (including pulse width and frequency, considered within the time parameter) increases the energy transferred to the treated medium. In the case of field strength, slight modifications square transferred energy. This fact opens up new possibilities for the use of PEF as a high-capacity heating system, thereby improving the possibilities of ohmic heating based on rapid and relatively uniform heating inside the food, similarly to microwaves or radio frequency, but with a higher penetration capacity in the product, and attaining an energetic efficiency close to 90% (Sastry, 2004). Moreover, the electroporabilizing effect of PEF would allow for an increase in the electrical conductivity of the product, thereby augmenting energy transfer while pulsing, and enabling a greater uniformity along the whole product, particularly if solid products are treated. For this purpose, moderate electric fields (MEF) using electric field

24 strengths up to 1 kV/cm are under research (Sastry, 2008, Kaur & Singh, 2016), as well as the limitation of
25 electrochemical reactions associated with the traditional application of ohmic heating (Samaranayake, Sastry,
26 & Zhang, 2005).

27 Recently, Timmermans et al. (2019) showed the microbial lethal effect of moderate-intensity Pulsed Electric
28 Fields by applying electric field strengths up to 5 kV/cm and 81°C to different fruit juices and by comparing
29 the effect to that of PEF at higher field strengths and to that of traditional heat treatments, respectively.
30 The application of moderate PEF intensities has shown less dependence on the pH of the treatment medium
31 and on the treated microbial species than PEF or heat, thus facilitating the implementation of moderate PEF
32 on an industrial level. Combined with the heating capacity of MEF applied to solid products, these benefits
33 can represent a new strategy to overcome the limitation of traditional heating of solid products, which results
34 in heterogeneous heat treatments, thereby affecting quality but, more importantly, reducing the uniformity of
35 microbial lethal effectiveness and thereby generating a **risk for food safety** (Yildiz-Turp, Sengun, Kendirci, &
36 **Icier, 2013**). Due to this, although ohmic heating and MEF can generate a relatively uniform heating effect,
37 this is a key point to be evaluated when applying heat treatments independently of the system. When ohmic
38 heating, MEF, and PEF are applied, temperature-dependent food properties such as electrical conductivity,
39 density, viscosity and thermal conductivity are modified. These changes may exert an influence on electric
40 field distribution and heating, thus compromising the treatment's uniformity and thereby the most important
41 criterion for a successful technology, which is safety. Thus, it is necessary to measure potential variation.
42 However, it is difficult to achieve experimental information regarding the distribution of electric field strength
43 and temperature in the treated product (Saldaña, Puertolas, Condon, Alvarez, & Raso, 2010).

44 Numerical simulation can provide detailed knowledge of the temporal and spatial distribution of the food's
45 electric field strength and temperature in the treatment chamber. With this information, an approach designed
46 to estimate the degree of microbial inactivation in an inhomogeneous MEF or PEF process can be implemented
47 if the heat resistance of the microorganisms of interest under isothermal conditions is known. Numerical
48 simulation has proven to be a very useful tool to optimize treatment chambers in ohmic, MEF, and PEF
49 treatments (Gerlach, Alleborn, Baars, Delgado, Moritz, & Knorr, 2008, Wölken, Sailer, Maldonado-Parra,
50 Horneber, & Rauh, 2017, Shim, Lee, & Jun, 2010, McLaren, Kopatz, Smith, & Jain, 2019). Research on the

51 microbial lethality of moderate-intensity PEF in solids due to Joule effect is nevertheless scarce. Moreover,
52 only a limited amount of information is available regarding the validation thereof by numerical simulation tools
53 that study the uniformity of both temperature and field strength in the treatment chamber, and regarding
54 the optimization of treatment conditions designed to achieve a certain level of inactivation of the pathogenic
55 microorganisms of interest. That is the objective of this investigation, which can serve as a starting point to
56 evaluate PEF technology as a further new system that can be applied to achieve rapid pasteurization of solid
57 products.

58 **2. Materials and methods**

59 The present study is two-fold. On the one hand, it was carried out a first set of PEF experiments on a solid
60 agar cylinder in order to evaluate the thermal effect of different field strengths on heating rates at different
61 distinct points within the solid, and on the inactivation of *Salmonella* Typhimurium 878. On the other hand,
62 a numerical model (Finite Element Model-FEM) was applied in order to predict the degree of ohmic heating
63 (OH) in the solid, thereby estimating the microbial inactivation of *Salmonella* Typhimurium 878 and evaluating
64 the uniformity of its lethality in the agar cylinder with the purpose of reducing the number of experiments in
65 laboratory. In order to estimate the degree of microbial inactivation, microbial thermal resistance at isothermal
66 conditions was determined.

67 *2.1. PEF system*

68 The PEF equipment used in this investigation was supplied by ScandiNova (Modulator PG, ScandiNova,
69 Uppsala, Sweden). The device generates square wave pulses of a width of 3 μs with frequencies varying from
70 0.5 to 300 Hz. The maximum output voltage and current are limited to 30 kV and 200 A, respectively. The
71 equipment consists of a direct current power supply which converts the 3-phase line voltage to a regulated DC
72 voltage. It charges up to six IGBT switching modules (high-power solid-state switches) to a primary voltage
73 around 1000 V. An external trigger pulse gates all the modules and controls their discharge to a primary pulsed
74 signal of around 1000 V. Finally, a pulse transformer converts the primary 1000 V pulse to a **3- μs high-voltage**
75 pulse of desired high voltage. For safe manipulation of the PEF device, and in order to obtain rectangular
76 **3- μs pulses**, the electric current delivered in the treatment chamber has to lie within a range of 80 to 150 A.

77 The treatment chamber consists of a cylindrical Teflon (polytetrafluoroethylene) tube closed with two polished
78 stainless steel cylinders of 20-mm diameter and 2-mm thickness, and separated 20-mm from each other where
79 the agar cylinder of 20-mm height and 20-mm diameter is located (Figure 1). To avoid movement of the
80 electrodes due to pressure when increasing temperature, two Teflon caps were screwed to the Teflon cylinder.
81 Three holes of 2-mm diameter in the cylindrical Teflon tube were used to introduce the temperature probes to
82 register the temperature at different locations of the agar cylinder. Actual voltage and current intensity applied
83 in the treatment chamber were measured with a high voltage probe (Tektronix, P6015A, Wilsonville, Oregon,
84 USA) and a current probe (Stangenes Industries Inc. Palo Alto, California, USA), respectively, connected to
85 an oscilloscope (Tektronix, TDS 220, Wilsonville, Oregon, USA)

86 [Figure 1 about here.]

87 2.2. PEF heating curves in agar

88 For benchmark, technical agar (Oxoid Basingstoke Hants, UK) was selected, since it is a product exhibiting
89 good clarity, controlled gelation and melting temperature, good diffusion characteristics, absence of toxic bac-
90 terial inhibitors, and relative absence of metabolically useful minerals and compounds. Different electrical and
91 thermal properties of the agar must be accounted for in ohmic heating generated by PEF. While its density
92 was assumed to be known $\rho = 998.2 \text{ (kg/mm}^3\text{)}$, its specific heat $c_p \text{ (J/kgK)}$ and its thermal conductivity k
93 (W/mK) were determined experimentally in our lab; their functional dependence on the temperature (Eq.(3)
94 and Eq.(2), respectively) was determined by linear regression (calibration not shown).

$$k(T) = -7.317 \cdot 10^{-1} + 7.322 \cdot 10^{-2} \cdot T - 9.492 \cdot 10^{-6} \cdot T^2 \quad (2)$$

$$c_p(T) = 3.991 \cdot 10^4 - 423.184 \cdot T + 1.879 \cdot T^2 - 3.716 \cdot 10^{-2} \cdot T^3 + 2.762 \cdot 10^{-6} \cdot T^4 \quad (3)$$

95 where T is the temperature of the agar.

96 In the case of the parameter of electrical conductivity, $\sigma \text{ (mS/cm)}$ Eq.(8), an experimental determination
97 thereof was performed due to its dependency on temperature, which varies, in turn, with the application of
98 PEF based on Eqs. (4) and (5):

$$T_f = T_0 + \frac{W_{total}}{4.18} \quad (4)$$

$$W_{total} = W_j \cdot N_{pulses} \quad (5)$$

99 where T_f and T_0 are the final and initial temperatures in °C, 4.18 is a conversion factor from Joules to calories,
 100 N_{pulses} is the number of squared pulses applied in the treatment, W_j (J/kg) the specific energy per pulse that
 101 is calculated from Eq. (6), and W_{total} is the total specific energy applied with the PEF treatment.

$$W_j = \frac{V \cdot I \cdot t_{eff}}{m} = \frac{V^2 \cdot \tau \cdot n}{GAP \cdot \pi \cdot r^2 \cdot \rho \cdot R} \quad (6)$$

102 where in the left term m is the mass of the product (kg), V is the applied voltage (V), I is the current
 103 intensity generated by the electric field applied (A), and t_{eff} is the effective time in which the the electric field
 104 is actually applied (s). In the right term, τ is the width of the pulse in which the electric field acts (s), n is the
 105 number of pulses, GAP is the distance between electrodes (length of the chamber in m), r is the radius of the
 106 electrodes (m), ρ is the density (kg/m^3), and R is the electrical resistance of the treatment chamber ($Ohms$,
 107 Ω) calculated as,

$$R = \frac{GAP}{\pi \cdot r^2 \cdot \sigma(T)} \quad (7)$$

108 in which the experimentally determined electrical conductivity σ finally appears.

109 From this analytical calculation, the relation between electrical conductivity, temperature, and the other
 110 electrical parameters becomes clear. Since for safe manipulation of the PEF device and to apply square wave
 111 pulses it is required to work with electric current within a range of 80 to 150 A, it was necessary to define
 112 the relationship of the electrical conductivity of the agar with temperature in order to apply PEF within the
 113 working conditions of the PEF system. The measurement of the electrical conductivity of the agar consisted
 114 in preparing technical agars of different electrical conductivities by boiling distilled water with powder agar
 115 and different concentrations of NaCl added. Once dissolved, temperature and electrical conductivity were
 116 measured at different temperatures (ranging between 50 and 90 °C) with a type-K thermocouple (Ahlborn

117 Almemo, Munich, Germany) and a conductivity probe (FYA641LFP1, Ahlborn Almemo) with temperature
 118 compensation connected to a data-logger (2590A, Ahlborn Almemo). With the obtained data, the following
 119 quadratic polynomial (response surface), Eq. (8) was generated by multiple regression analysis to ascertain the
 120 effect of temperature (T) and percentage of NaCl ($[\%]_{salt}$) on electrical conductivity $\sigma(T)$ using the Design-
 121 Expert 6.0.6 software package (Stat-Ease Inc. Minneapolis, MN, USA):

$$\begin{aligned} \sigma(T) = & -3.269 \cdot 10^{-1} + 1.044 \cdot 10^{-2} \cdot T + 9.250 \cdot [\%]_{salt} + 2.940 \cdot 10^{-1} \cdot T \cdot [\%]_{salt} \\ & + 2.42 \cdot [\%]_{salt}^2 + 1.330 \cdot 10^{-3} \cdot T^2 \cdot [\%]_{salt} - 3.951 \cdot 10^{-2} \cdot T \cdot [\%]_{salt}^2 \end{aligned} \quad (8)$$

122 Based on this equation, for a PEF working current intensity of 80 A, an initial temperature of 23 °C in the
 123 agar, and an approximated initial electrical conductivity of 0.373 S m⁻¹, the required concentration of salt is
 124 0.24%. In this way, the electrical conductivity of the sample is controlled to avoid exceeding 150 A by the end
 125 of the PEF treatments. To evaluate the temperature in different locations of the agar cylinders, a technical
 126 agar cylinder of 10-cm height and 10-cm diameter with 0.24% added NaCl was prepared. From this large
 127 cylinder, and using a hole puncher of 2-cm of diameter, small agar cylinders were obtained and cut in pieces
 128 of 2-cm height, which were subsequently introduced in the treatment chamber. For each PEF treatment, an
 129 agar cylinder was introduced in the treatment chamber contacting both electrodes. Three 1-mm-diameter fiber
 130 optic probes model TPT-62-BA-C7-F2-M2-R1-ST (Fiberoptic Components, USA) were introduced through
 131 three holes of 2-mm diameter with the purpose of registering the temperature at different locations of the agar
 132 cylinder. Figure 2 shows the different locations at which probes were located: i.e., at the center of the cylinder
 133 (P2), at the center of the cylinder and 1-mm from the transition between the electrode and the sample (P1), or
 134 at 1-mm from the transition between the sample, the electrode, and the Teflon cylinder (P4). The evolution of
 135 temperature at the different locations was recorded to evaluate the amount of heating produced when applying
 136 pulses of different electric field strengths (2.5 to 3.75 kV/cm) and number of pulses (10 to 3000 pulses) through
 137 time (pulses applied up to a maximum of 60 seconds) at a frequency of 50 Hz. Heating rates (expressed as the
 138 increase in number of degrees Celsius per second of PEF treatment, °C/s) for each PEF treatment condition at
 139 each location were determined from the slope of the relationship between the temperatures of the PEF-treated

140 agar cylinder and heating time.

141 [Figure 2 about here.]

142 2.3. Microbial inactivation by thermal treatments

143 The strain of *Salmonella* Typhimurium 878 used in this investigation was supplied by the Spanish Type
144 Culture Collection. In the course of this investigation, the culture was maintained on slants of Tryptic Soy Agar
145 (Biolife, Milan, Italy) with 0.6% Yeast Extract added (Biolife) (TSAYE). A broth subculture was prepared by
146 inoculating a test tube containing 5 mL of Tryptic Soy Broth (Biolife) with 0.6% Yeast Extract (TSBYE) with a
147 single colony, followed by incubation at 37°C for 24 h. With this subculture, a flask containing 50 mL of sterile
148 TSBYE was inoculated to a final concentration of approximately 10^6 cells/mL. The culture was incubated under
149 agitation at 37 °C until the stationary growth phase was reached (24 h), achieving a concentration of $2 \cdot 10^9$
150 CFU/mL (data not shown). This suspension was used to define the heat resistance of *Salmonella* Typhimurium
151 at isothermal conditions in buffers, and when treated by PEF in agar cylinders.

152 2.3.1. Microbial inactivation at isothermal conditions

153 In order to estimate the microbial inactivation that could be achieved in the different monitored temper-
154 ature positions of the agar cylinder when applying PEF, heat resistance of *Salmonella* Typhimurium 878 was
155 determined at isothermal conditions. For this, heat treatments were carried out in a thermoresistometer TR-SC
156 (Condon, Lopez, Oria, & Sala, 1989, Condon, Arrizubieta, & Sala, 1993) in which microorganisms were treated
157 at constant temperatures ranging from 55 to 64°C in sterilized pH 6.8 McIlvaine citrate-phosphate buffer. Once
158 the treatment medium was tempered, 0.2-mL of the microbial suspension was inoculated into the treatment
159 medium. At different heating times, 0.1-mL samples were collected and immediately pour-plated. Survival
160 curves (decimal logarithm of the number of surviving microorganisms vs. heating time) were obtained at differ-
161 ent investigated temperatures. From the obtained survival curves, the traditional decimal reduction time value
162 (D_t value), i.e., the time to inactivate 90% of the microbial population, and the z value, i.e., the temperature
163 increase to reduce the D_t value by 90%, were calculated.

164 Based on the heating rates obtained when PEF treatments were applied, temperatures at different points of
165 the agar through time (non-isothermal treatments) were estimated. The estimated survival curves corresponding

166 to non-isothermal treatments at the corresponding point of the agar cylinder were calculated by integrating the
167 lethal effect of the different temperatures for each treatment time (L value) and applying the following equation:

$$L = \int_0^{t'} \frac{t}{D_{T_{ref}} \cdot 10^{\frac{T_{ref}-T}{z}}} \cdot dt \quad (9)$$

168 where t' is the PEF heating time (in seconds), and $D_{T_{ref}}$ is the D_t value at a reference temperature (T_{ref}): in
169 this investigation, 60°C, obtained under isothermal conditions.

170 2.3.2. Microbial inactivation in solid agar

171 In order to validate the estimated microbial inactivation based on Eq. 9, the lethality of PEF treatments
172 in agar cylinders was determined. For this purpose and prior to treatments, 1 mL of the microbial suspension
173 was added to 1 L of sterilized technical agar with 0.24% NaCl when the liquid agar was at 47 °C, which is
174 not lethal for the pathogen but allows for a homogeneous distribution of the population over the entire sample.
175 Subsequently, the agar was cooled down until gelification. With a sterile hole puncher of 2-cm of diameter,
176 small agar cylinders were obtained and cut in pieces of 2-cm height, which were introduced in the treatment
177 chamber. Two sets of experimental conditions designed to investigate the influence of temperature on microbial
178 inactivation by PEF were applied: i) 2.5 kV/cm electrical field strength, 3000 squared pulses of 3 μ s, at a
179 frequency of 50 Hz during 60 seconds; ii) 3.75 kV/cm electrical field strength, 3000 pulses of 3 μ s at a frequency
180 of 50 Hz during 60 seconds. After treatments, the agar cylinder was extracted from the treatment chamber
181 in sterile conditions. Pieces of 0.2 g of agar from positions P2 and P4 were added to 1 mL of sterile 0.1%
182 peptone water, homogenized, and 0.1 mL thereof were plated onto TSAYE. Plates were incubated at 37 °C for
183 24 h, after which colonies were counted with an improved image analyzer automatic counter (Protos, Analytical
184 Measuring Systems, Cambridge, UK) as described elsewhere (Condon et al., 1996). Survival curves were based
185 on mean values obtained from three independent experiments.

186 2.4. Finite Element model for ohmic heating

187 A coupled thermo-electrical problem is involved in ohmic heating. On the one hand, Laplace equations solve
188 the intensity of the electric field applied over the domain. On the other hand, Joule's equation determines
189 the internal energy generated by the electric field. According to Joule's equation, the heat generated Q (J)

190 during ohmic heating is proportional to the square of the electrical current that flows through the sample, its
191 resistance, and the time in the course of which such current is flowing.

192 The governing equation for heat transfer is,

$$\rho c_p(T) \frac{\partial T}{\partial t} - \nabla \cdot (k(T) \nabla T) = Q \quad (10)$$

193 where ρ is the density of the solid, $c_p(T)$ is the specific heat, and $k(T)$ is the thermal conductivity. The term,
194 Q is the the conversion of electrical to thermal energy (Joule heating),

$$Q = \sigma(T) \mathbf{E}^2 \quad (11)$$

195 where \mathbf{E} denotes the electric field strength. It is assumed that the pulsating electric field does not induce a
196 time varying magnetic field, thus $\nabla \times \mathbf{E} = 0$. As a consequence, the electric field vector \mathbf{E} can be written as the
197 gradient of the electrical potential V ,

$$\mathbf{E} = -\nabla V \quad (12)$$

198 Based on charge conservation, the governing equation for the electrical potential can be written as

$$\nabla \cdot \mathbf{J} = \nabla \cdot [\sigma(T) \nabla V] = 0 \quad (13)$$

199 with \mathbf{J} denoting the current density.

200 The coupled differential problem can be solved by the finite element method. To simulate ohmic heating,
201 we developed an axisymmetric model using the commercial software Abaqus (Dassault Systèmes). The model
202 includes three different parts: the electrodes of variable cross-section (radius of 10-mm and thickness of 2-
203 mm), the plastic container that houses the agar and the electrodes, and the treatment chamber containing the
204 technical agar with 20-mm diameter and 20-mm length (Figure 3.a). The number of nodes and elements for
205 discretization of the domain were 3,321 and 1,050, respectively. The model was meshed with 8-node quadrilateral
206 finite elements with quadratic approximation (DCAX8E).

207 [Figure 3 about here.]

208 Material properties for the agar were the ones described previously, presenting dependence on temperature
209 for electrical (σ) and thermal (k) conductivity and specific heat (c_p). Material properties for electrodes were
210 those of stainless steel and for the plastic envelope those of teflon (Table 1).

211 [Table 1 about here.]

212 Two different types of boundary conditions were introduced in the model: electrical and thermal.

213 First, the electric potential between electrodes was defined by setting one electrode as the voltage electrode
214 (in blue in Figure 3.b) and the other as the ground electrode (in green in Figure 3-b). The load amplitude of
215 the electric pulse was the same as the one used in the commercial PEF device, i.e., a squared electrical pulse
216 of $3 \mu s$ of duration, a given number of pulses, frequency, and total duration of the experiment. Knowing this,
217 each calculation step has a plateau of $3 \mu s$ in which the electric pulse is set to the highest voltage (i.e., 5 kV
218 – 2.5 kV/cm – or 7 kV – 3.75 kV/cm – depending on the experiment under analysis), followed by a valley of
219 variable duration (i.e., depending on the number of pulses, frequency, and duration of the experiment) in which
220 no electric field is applied.

221 Secondly, a condition of natural convection was set in the boundary of the domain in order to allow the heat
222 to be transferred to the surrounding media and to allow the sample to cool down. Natural convection boundary
223 conditions depend on the difference between the temperature in the surrounding media and the domain, and
224 a coefficient of heat transfer h (W/mK). For air, values for h in natural convection are relatively low; in this
225 study, they were set to $h = 5W/mK$. Finally, the initial temperature was $T_0^{Agar} = 23 \text{ }^\circ\text{C}$ for the technical agar,
226 $T_0 = 25 \text{ }^\circ\text{C}$ for the electrodes, and $T_0 = 25 \text{ }^\circ\text{C}$ for the plastic container. Simulated temperatures were recorded
227 at the points at which the real probe should be located in the experiments: i) at the center of the treatment
228 chamber (P2); and ii) at 1-mm from the transition between the sample, electrode, and plastic cylinder (P4).

229 For the sake of simplicity and computational effort, we assume that the treatment chamber presents a perfect
230 symmetry of revolution (i.e., the use of an axisymmetric model); the control unit is able to deliver perfect
231 continuum pulses during all the treatment; the material behavior is perfectly homogeneous and there is not air
232 entrapped, nor gaps between the electrodes and the agar; and that the probes do not affect the conductivity

233 and/or electric field during measurement. Despite these assumptions, there is not lack of generality in the
234 present benchmark study.

235 3. Results and Discussion

236 This study was the first to evaluate microbial inactivation via PEF treatments in a solid product based on
237 generated ohmic heating, considering *Salmonella* Typhimurium as reference. Moreover, inactivation in a solid
238 (an agar cylinder) has been estimated based on the isothermal heat resistance of *Salmonella* Typhimurium after
239 the application of PEF treatments and the time-temperature distribution predictions obtained by numerical
240 simulation tools, after which the results of the actual microbial inactivation were validated. As indicated, it
241 was necessary to define the ohmic heating rates in the agar cylinder used as a reference solid material when
242 applying PEF under different conditions in order to define the hottest and coldest point to which the results
243 refer. These rates were estimated via computational simulation by predicting temporal space distribution of the
244 temperature, a procedure that is essential in order to predict distribution in a static ohmic heating chamber,
245 for example, and to optimize ohmic heating processes (Knoerzer, Regier, & Schubert, 2006).

246 3.1. Experimental results for ohmic heating and microbial inactivation

247 In a first step, temperature increment in the different tested points of the agar cylinder when applying
248 PEF treatments of 2.5 kV/cm at 50 Hz was evaluated (Figure 4). Linear relationship between processing time
249 (number of pulses multiplied by pulse frequency) and temperature increase were described. As observed, points
250 P2, P5 and P6 were the ones with the highest heating rates (1.14 ± 0.04 , 1.28 ± 0.08 , 1.16 ± 0.06 °C/s), while
251 points P1 and P4 were the ones with the lowest (0.99 ± 0.02 , 0.95 ± 0.03 °C/s). There were no statistically
252 significant differences ($p=0.05$) among slopes, even comparing positions (P4 and P5) with the most distinct
253 values, but differences of almost 10 °C were determined after 20 seconds of treatment among the hottest and
254 the coldest points. This means that the longer the treatment time, the lesser the uniformity of temperature
255 in the cylinder. Considering this last appreciation and in order to evaluate the effect of the different heating
256 rates in terms of lethality, *Salmonella* Typhimurium inactivation was evaluated in position P4, the coldest
257 point, after applying PEF treatments of different duration. Also, position P2 (the central point of the agar
258 cylinder), which presented one of the highest heating rates, was selected to compare results and to evaluate the

259 uniformity of heating. It has to be pointed out that position P4, and also position P1, i.e., the ones with the
260 lowest heating rates, were located close to the high voltage electrode. Similar observations have been reported
261 in literature indicating a cold zone at the junction of electrodes in ohmic heating treatments (Marra, 2014).
262 The occurrence of these cold zones is a noticeable limitation of PEF technology in terms of its application to
263 design pasteurization or even sterilization treatments.

264 [Figure 4 about here.]

265 In order to evaluate the lethality of PEF in positions P2 and P4, the heating rates shown in Figure 4 were
266 used to estimate temperature fluctuation over time when applying PEF at 2.5 kV/cm and 50 Hz (Figures 5.a
267 and 5.b for positions P2 and P4, respectively). Also, and since ohmic heating is proportional to the square of
268 electric field strength (Eq. 1), temperature increase was evaluated at a higher field strength of 3.75 kV/cm and
269 50 Hz (Figures 5.c and 5.d for positions P2 and P4, respectively). In this case, heating rates were 2.52 ± 0.34
270 and 2.15 ± 0.22 °C/s for positions P2 and P4 respectively.

271 Based on these time-temperature profiles and on a $D_{60^\circ C}$ value of $0.39 \pm 0.04'$ and a z value of 5.0 ± 0.1
272 °C obtained from the thermal inactivation of *Salmonella* Typhimurium at isothermal conditions in McIlvaine
273 buffer of pH 6.8 (data not shown), Figure 5 was plotted for P2 (Figure 5.a and 5.c) and P4 (Figure 5.b and
274 5.d) for treatments at 2.5 and 3.75 kV/cm. In this figure, the average (dotted lines), and the maximum and
275 minimum theoretical temperatures (pink zone) when applying PEF were calculated based on heating rates. The
276 theoretical inactivation of *Salmonella* Typhimurium (continuous line) was calculated using (9). In this graph,
277 the rate of inactivation for the maximum and minimum temperatures after a given PEF treatment (blue zone)
278 was also calculated. As observed, inactivation speed was faster the higher the temperature, and it was more
279 rapid in position P2 than in P4 at both field strengths.

280 In the case of 2.5 kV/cm, after 48 seconds of PEF treatments 5- \log_{10} cycles of *Salmonella* Typhimurium
281 were inactivated in the center of the cylinder (Figure 5.a), whereas in the best-case scenario only two cycles
282 were inactivated at a distance of 1-mm from the high voltage electrode (Figure 5.b), thereby registering mean
283 temperatures of 73 °C (maximum 78 °C) and 63 °C (maximum 73 °C), in positions P2 and P4, respectively.
284 To achieve 5- \log_{10} cycles of inactivation near the electrode, heating time had to be increased to 58 seconds
285 by applying 2900 pulses of 3 μs , reaching mean temperatures of 75 °C in the worst-case scenario. In Figure

286 5, the uniformity of the PEF treatments depending on location can likewise be easily observed. Thus, for an
287 average 5- \log_{10} reduction of the microbial population, 44 and 50 s would be required in positions P2 and P4,
288 respectively, thereby determining possible variations in temperature in those locations from 64 to 73 °C (9 °C)
289 in position P2 and from 62 to 75 °C (13 °C) in position P4. From a practical point of view, such a variation
290 in temperature and heating rates would imply a variation in processing time of 8 seconds (from 40 to 48 s)
291 and 14 seconds (from 44 to 58 s) in positions P2 and P4, respectively, in order to achieve 5- Log_{10} -reductions of
292 *Salmonella* Typhimurium.

293 When evaluating the effect of electric field strength, conclusions similar to those reached at 2.5 kV/cm can be
294 obtained at 3.75 kV/cm, but with more rapid temperature increment and microbial inactivation. Thus, 5- \log_{10}
295 reductions were obtained after 29 seconds of treatment (a 50% reduction of processing time for a 1 kV/cm
296 increase in field strength) independently of location, with less variation in time for this level of inactivation,
297 requiring from 18 to 23 seconds (5 s) and from 20 to 29 seconds (9 s) in positions P2 and P4, respectively. These
298 results seem to indicate a higher uniformity in temperature distribution when electric field strength is increased.
299 However, when measuring temperature experimentally, the variation of this parameter seems to be larger than
300 when applying 2.5 kV/cm. Thus for an average 5- \log_{10} microbial reduction at 3.75 kV/cm, temperature varied
301 from 63 to 75 °C (12 °C after 19.5 s) in position P2 and from 60 to 79 °C (19 °C after 23 s) in position P4,
302 respectively, which was higher than when PEF was applied at 2.5 kV/cm. These results would indicate that the
303 faster the heating rate, the higher the uncertainty when measuring temperature experimentally, whereby the
304 variability of measurements increases depending on small variations in the measurement point. This uncertainty
305 is reflected in a wider range of temperatures (red zone in Figure 5) due to a higher variability in heating rates
306 calculated from the experimental measurements (95% confidence limits of the heating rates at 3.75 kV/cm were
307 larger – e.g. 0.34 and 0.22 – than for 2.5 kV/cm – from 0.02 to 0.08).

308 In order to evaluate in more detail this possible influence of uncertainty regarding the location of the probe
309 when measuring the temperature, numerical simulation tools can be of great interest, as will be discussed later
310 on. In order to validate these results, Figure 5 also includes the actual inactivation of *Salmonella* Typhimurium
311 obtained in positions P2 and P4 after different PEF treatments at both field strengths (marked with stars in
312 Figure 5). As observed, the estimated degree of microbial inactivation agrees with the Log_{10} reductions observed

313 at both locations and field strengths: the most intense PEF treatments achieve 5- \log_{10} reductions, and even
314 situations without any detectable microbial growth (reductions of an order of more than 6- \log_{10}). Inactivation
315 was only slightly underestimated for the treatments at 3.75 kV/cm and position P2, which was the one with
316 the highest variability in heating rates. The agreement between estimated and real inactivation would indicate
317 that heat resistance obtained under isothermal conditions can adequately predict the inactivation of *Salmonella*
318 Typhimurium under non-isothermal conditions, which occur when PEF is applied. This agreement could be
319 explained by the supposition that high heating rates would limit the possible occurrence of thermal adaptation
320 of *Salmonella*, as has been observed for other microorganisms such as *Listeria monocytogenes* at lower heating
321 rates under standard heat treatments (Monfort et al., 2012).

322 On the other hand, this concordance between estimated and observed microbial inactivation would also in-
323 dicate that PEF treatments applied at the studied field strengths would not produce any additional inactivation
324 than that generated by a heat treatment. In other words, the applied field strength would not be sufficient to
325 produce irreversible electroporation, or to sensitize *Salmonella* Typhimurium to the applied temperatures, as
326 has been observed at higher field strengths (Saldaña et al., 2010). These results are not in agreement with those
327 obtained by other authors, who achieved an additional inactivation by electroporation even at low field strengths
328 (Machado, Pereira, Martins, Teixeira, & Vicente, 2010, Park & Kang, 2013). This could be associated with a
329 possible reversible electroporation which could become irreversible by means of heating, thereby increasing the
330 treatment's overall lethality (Kim, Choi, & Kang, 2017). That difference in observed behavior could be ascribed
331 to the fact that those results were obtained in liquid media, in which ohmic heating might generate undesired
332 electrochemical species that lead to inactivation, as pointed out (Timmermans et al., 2019). Electrochemical
333 reactions take place at the interface between the electrode and the liquid. In this investigation, that effect could
334 be taking place, but since a solid medium was used, the potentially generated electrochemical species would
335 remain in the interface, not affecting the entire treated product as would occur in a liquid medium.

336 [Figure 5 about here.]

337 3.2. Temperature and inactivation predictions of the mathematical model

338 The obtained results show the potential of PEF for microbial inactivation in solid products. However, as the
339 evaluation of the effect of PEF parameters on temporal and spatial distribution of electric field strength and

340 temperature, and thus likewise of the degree of microbial inactivation, are all difficult to measure. Numerical
341 simulation provides us with an adequate tool to obtain this information, permitting a confirmation of the
342 experimental results and, in this case the detection of the coldest point in the treatment zone. Figure 6 shows
343 the finite element simulation of ohmic heating resulting when a PEF treatment (2.5 kV/cm at 50 Hz) is applied
344 in the treatment chamber, presenting results of temperature gradient (Figure 6.a), heat transfer (Figure 6.b),
345 and electric potential (Figure 6.c). As observed, numerical simulations support the hypothesis that, although
346 electric potential is homogeneous and linear in the sample (Figure 6.c), the distribution of temperature presents
347 a gradient of up to 10 °C towards the periphery (Figure 6.a), thereby representing a risk factor to account for
348 in the context of PEF treatments. This could be probably be ascribed to heat transfer (Figure 6.b), which is
349 mostly focalized in the electrodes due to the high thermal conductivity of stainless steel, whereby the chamber
350 is almost adiabatic due to its plastic components.

351 [Figure 6 about here.]

352 Nevertheless, predictions of numerical simulations were in good agreement with experimental temperature
353 ranges and inactivation values. Thus, Figure 7 plots simulated temperature increments and microbial inacti-
354 vation in positions P2 (Figure 7.a and 7.c) and P4 (Figures 7.b and 7.d) after the application of PEF at 2.5
355 kV/cm and 50 Hz (Figures 7.a and 7.b), and at 3.75 kV/cm and 50 Hz (Figures 7.c and 7.d). Lines indicate the
356 predictions, and shaded areas represent the experimental ranges previously shown in Figures 5. As observed,
357 simulated temperatures in the technical agar (black and blue solid lines in Figure 7) fell inside the experimental
358 ranges for the center (position 2) and the ‘corner’ of the treatment chamber (position 4). Moreover, predicted
359 inactivation based on simulated temperatures fell inside the experimental range (grey shaded areas in Figure
360 7).

361 Interestingly, models help to outline the measuring system’s high sensitivity to the location of the probe,
362 which could help explain the high variability in some of the experimental measurements. Simulated temper-
363 atures (black and blue solid lines in Figure 7) correspond to the same spatial location within the treatment
364 chamber (positions P2 and P4), with a slight perturbation of 0.5-mm around the measuring point. This small
365 perturbation, which simulates the uncertainty in the positioning of the temperature probe, shows that it is
366 extremely important to ensure a precise measuring protocol in order to properly determine the gradient in the

367 temperature field within the sample. This is more important the higher the heating rate, in our case when a
368 more intense PEF treatment was applied (3.75 kV/cm). In the simulations, it seemed that a lesser degree of
369 variability was to be estimated when a higher field strength was applied at both locations. That variability can
370 be observed in more detail in Figure 8, which features the correlation between the experimental final tempera-
371 tures in the chamber (P2 and P4) and the simulated final temperature after the application of PEF treatments
372 at 2.5 and 3.75 kV/cm.

373 As observed, although occasionally the experimental temperature is slightly overestimated, simulated tem-
374 peratures lie within a suitable range and, thus, models can be used to explore different treatments without
375 having to recur to experimental benchwork. Vertical error-bars in Figure 8 show the degree of uncertainty
376 in experimental measurements, and horizontal error-bars indicate the uncertainty in numerical measurements
377 (for experiments of different treatment times). As observed, numerical models showed that the uncertainty in
378 temperature due to the uncertainty in the positioning of the temperature probe was higher in P4 (the zone
379 close to the electrode) than in P2 (center) and, again, that a higher electric potential helped to reduce the
380 gradient of temperature thanks to shorter application times. That is, the application of pulses of higher electric
381 field strength would result in a more homogeneous temperature distribution by limiting the release of heating
382 through electrodes.

383 [Figure 7 about here.]

384 [Figure 8 about here.]

385 4. Conclusions

386 This study demonstrated the potential of PEF as a system capable of rapidly achieving microbial inactivation
387 in solid products thanks to a higher heat capacity transfer when applying field strengths over 1 kV/cm. Based
388 on our knowledge, this is the first study on this particular aspect, and it was possible to reduce 5 or even more
389 \log_{10} cycles of *Salmonella* Typhimurium 878 in solid agar with treatment times below 1 minute. These results
390 indicated that PEF could be further investigated and considered as an alternative to traditional conductive
391 heat treatments for microbial inactivation. However, gradients of up to 10 °C were determined between the
392 hottest and coldest point which is located in the interphase zone between agar and the high voltage electrode.

393 The consequence is a need for experimental times with delays of around 10 seconds to ensure a certain level of
394 microbial inactivation. Therefore, it is essential to evaluate the effect of PEF parameters on heating rates and
395 temperature uniformity. For that evaluation, numerical models proved to be a useful tool. Based on the obtained
396 simulations, increasing electric field strength reduced processing time (an increment of 1 kV/cm resulted in half
397 processing time, i.e., 58 to 29 seconds), as well as the temperature distribution in the agar cylinder, thereby
398 improving treatment uniformity and, consequently, the degree of microbial inactivation. However, more research
399 is necessary in order to evaluate the effect not only of electric field strength but of pulse width, frequency, and
400 other factors on temperature and microbial inactivation uniformity in the entire solid.

401 **Acknowledgements**

402 The authors thank A. Picardo for his help in designing and constructing the PEF treatment chamber.

403 The authors gratefully acknowledge research support from the Spanish Ministry of Economy and Com-
404 petitiveness (Grant GL2017-84084-R and DPI2017-84047-R) and the Department of Industry and Innovation
405 (Government of Aragón) through Research Group Grant T24-17R and A03-17R (cofinanciado con Feder 2014-
406 2020: Construyendo Europa desde Aragón).

407 The authors also acknowledge assistance provided by CIBER-BBN, an initiative funded by the VI National
408 R & D & i Plan 2008-2011, Iniciativa Ingenio 2010, Consolider Program, CIBER Actions, and financed by the
409 Instituto de Salud Carlos III with assistance from the European Regional Development Fund.

410 **References**

411 Barbosa-Canovas, G. V., Fernandez-Molina, J. J., Swanson, B. G., 2001. Pulsed electric fields: A novel tech-
412 nology for food preservation. *Agro Food Industry Hi-Tech* 12 (2), 9–14.

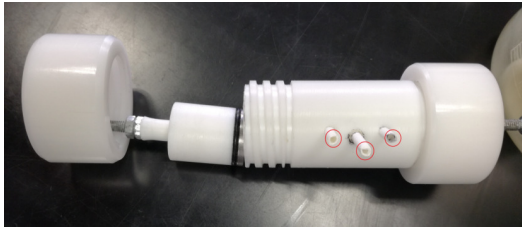
413 Buckow, R., Ng, S., Toepfl, S., September 2013. Pulsed electric field processing of orange juice: A review on
414 microbial, enzymatic, nutritional, and sensory quality and stability. *Comprehensive Reviews in Food Science*
415 *and Food Safety* 12 (5), 455–467.

- 416 Condon, S., Arrizubieta, M. J., Sala, F. J., 1993. Microbial heat-resistance determinations by the multipoint
417 system with the thermoresistometer TR-SC - improvement of this methodology. *Journal of Microbiological*
418 *Methods* 18 (4), 357–366.
- 419 Condon, S., Lopez, P., Oria, R., Sala, F. J., 1989. Thermal death determination - design and evaluation of a
420 thermoresistometer. *Journal of Food Science* 54 (2), 451–457.
- 421 Condon, S., Palop, A., Raso, J., Sala, F. J., 1996. Influence of the incubation temperature after heat treatment
422 upon the estimated heat resistance values of spores of *Bacillus subtilis*. *Letters in Applied Microbiology* 22 (2),
423 149–152.
- 424 Gerlach, D., Alleborn, N., Baars, A., Delgado, A., Moritz, J., Knorr, D., 2008. Numerical simulations of pulsed
425 electric fields for food preservation: A review. *Innovative Food Science and Emerging Technologies* 9 (4),
426 408–417.
- 427 Kaur, N., Singh, A. K., 2016. Ohmic heating: Concept and applications-a review. *Critical Reviews in Food*
428 *Science and Nutrition* 56 (14), 2338–2351.
- 429 Kim, S.-S., Choi, W., Kang, D.-H., 2017. Application of low frequency pulsed ohmic heating for inactivation
430 of foodborne pathogens and ms-2 phage in buffered peptone water and tomato juice. *Food Microbiology* 63,
431 22–27.
- 432 Knoerzer, K., Regier, M., Schubert, H., 2006. Microwave heating: A new approach of simulation and validation.
433 *Chemical Engineering and Technology* 29 (7), 796–801.
- 434 Machado, L. F., Pereira, R. N., Martins, R. C., Teixeira, J. A., Vicente, A. A., 2010. Moderate electric fields
435 can inactivate *Escherichia coli* at room temperature. *Journal of Food Engineering* 96 (4), 520–527.
- 436 Marra, F., 2014. Mathematical model of solid food pasteurization by ohmic heating: Influence of process
437 parameters. *Scientific World Journal* 2014 (236437).
- 438 McLaren, C. T., Kopatz, C., Smith, N. J., Jain, H., 2019. Development of highly inhomogeneous temperature
439 profile within electrically heated alkali silicate glasses. *Scientific Reports* 9 (2805).

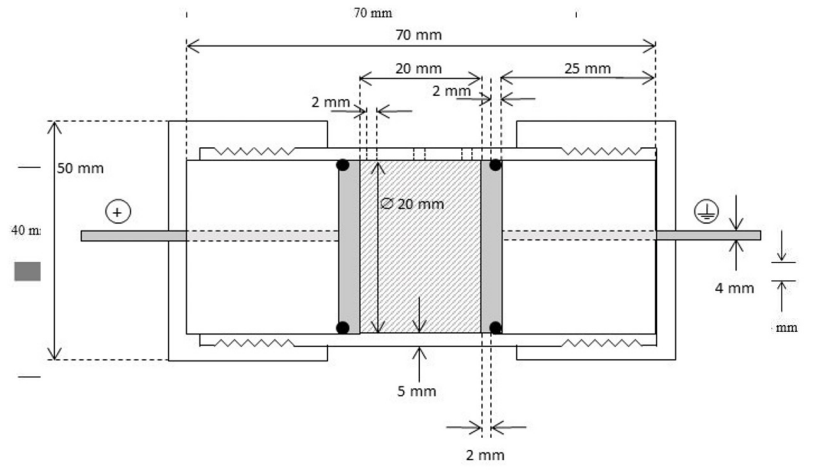
- 440 Monfort, S., Sagarzazu, N., Gayan, E., Raso, J., Alvarez, I., 2012. Heat resistance of *Listeria* species to liquid
441 whole egg ultrapasteurization treatment. *Journal of Food Engineering* 111 (2), 478–481.
- 442 Park, I.-K., Kang, D.-H., 2013. Effect of electropermeabilization by ohmic heating for inactivation of *Escherichia*
443 *coli* O157:H7, *Salmonella enterica* Serovar *Typhimurium*, and *Listeria monocytogenes* in buffered peptone
444 water and apple juice. *Applied and Environmental Microbiology* 79 (23), 7122–7129.
- 445 Saldaña, G., Puertolas, E., Condon, S., Alvarez, I., Raso, J., 2010. Modeling inactivation kinetics and occurrence
446 of sublethal injury of a pulsed electric field-resistant strain of *Escherichia coli* and *Salmonella Typhimurium*
447 in media of different ph. *Innovative Food Science and Emerging Technologies* 11 (2), 290–298.
- 448 Samaranyake, C. P., Sastry, S. K., Zhang, H., 2005. Pulsed ohmic heating - a novel technique for minimization
449 of electrochemical reactions during processing. *Journal of Food Science* 70 (8), E460–E465.
- 450 Sastry, S., 2008. Ohmic heating and moderate electric field processing. *Food Science Technology International*
451 14 (5), 419–422.
- 452 Sastry, S. K., 2004. *Advances in ohmic heating and moderate electric field (MEF) processing*. CRC Press.
- 453 Sastry, S. K., Li, Q., 1996. Modeling the ohmic heating of foods. *Food Technology* 50 (5), 246–248.
- 454 Shim, J., Lee, S. H., Jun, S., 2010. Modeling of ohmic heating patterns of multiphase food products using
455 computational fluid dynamics codes. *Journal of Food Engineering* 99 (2), 136–141.
- 456 Timmermans, R. A. H., Mastwijk, H. C., Berendsen, L. B. J. M., Nederhoff, A. L., Matser, A. M., Van Boekel,
457 M. A. J. S., Groot, M. N. N., 2019. Moderate intensity pulsed electric fields (PEF) as alternative mild
458 preservation technology for fruit juice. *International Journal of Food Microbiology* 298, 63–73.
- 459 Wölken, T., Sailer, J., Maldonado-Parra, F. D., Horneber, T., Rauh, C., 2017. Application of numerical simu-
460 lation techniques for modeling pulsed electric field processing. *Handbook of electroporation*, 1–31.
- 461 Yildiz-Turp, G., Sengun, I. Y., Kendirci, P., Icier, F., 2013. Effect of ohmic treatment on quality characteristic
462 of meat: A review. *Meat Science* 93 (3), 441–448.

| | Stainless steel | Teflon |
|------------------------------------|-------------------|------------|
| k (W/mK) | 12 | 0.25 |
| σ (S/m) | $1.45 \cdot 10^6$ | 10^{-24} |
| c_p ($J \cdot kg^{-1} K^{-1}$) | 502 | 2,200 |
| ρ (kg/m^3) | 7,850 | 970 |

Table 1: Properties for stainless steel and teflon.



(a)



(b)

Figure 1: Treatment chamber used in the experimental set-up. (a) Photograph. (b) Scheme and dimensions.

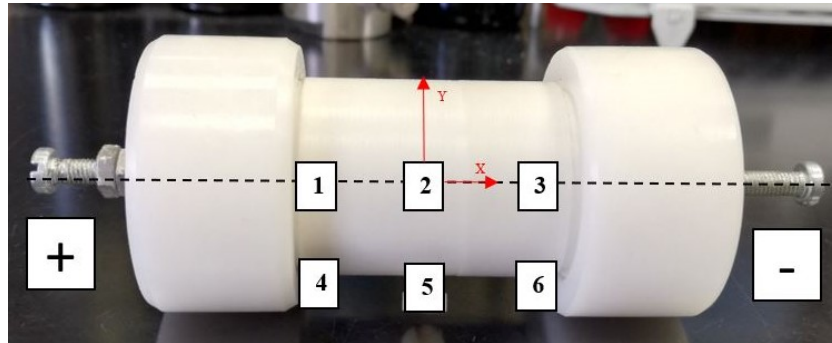
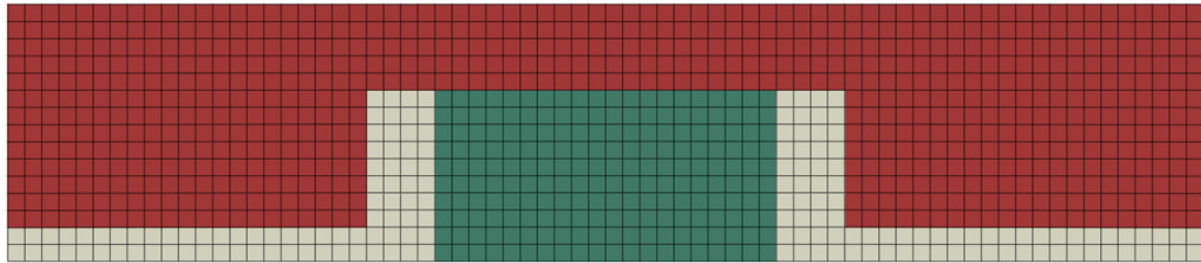
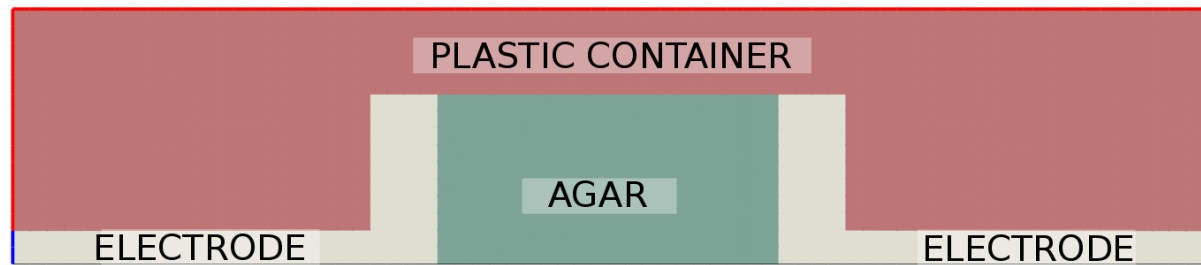


Figure 2: Location of the different temperature-measurement points in the PEF treatment chamber.



(a)

HEAT TRANSFER TO AIR
(NATURAL CONVECTION)



(b)

Figure 3: A finite element model of ohmic treatment. (a) Discretization of the domain including electrodes, plastic envelope, and agar; (b) Boundary conditions for the resolution of the coupled thermo-electrical problem.

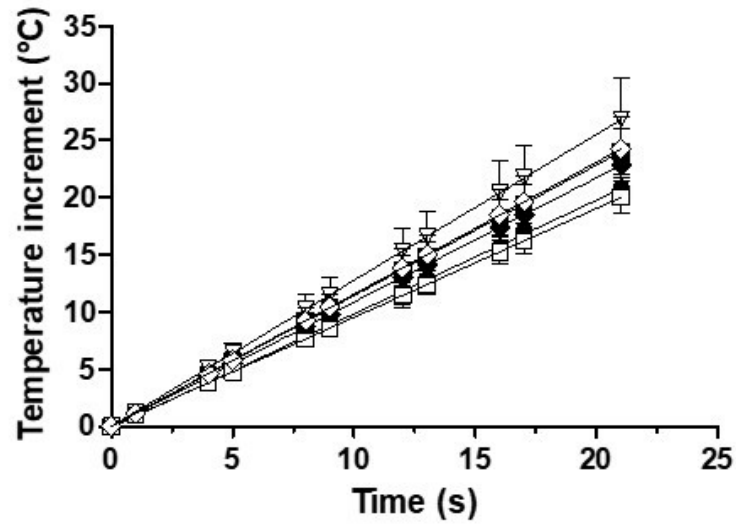


Figure 4: Increase in the temperature of the agar when applying PEF treatments of 2.5 kV/cm at 50 Hz at different positions of the agar: P1 (●), P2 (■), P3 (▲), P4 (○), P5 (□), and P6 (△).

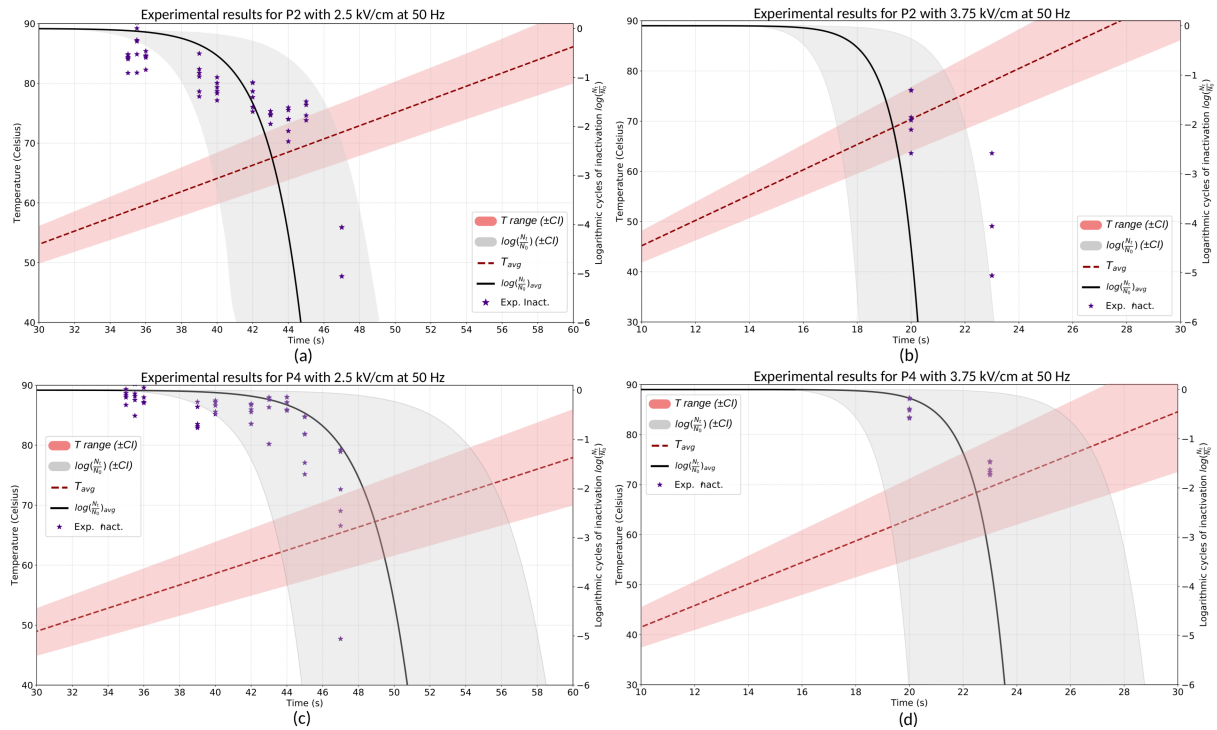


Figure 5: Results of experimental inactivation (inactivation showed in purple stars) and theoretical evolution of temperature (reddish palette) and inactivation (grayscale palette) of *Salmonella Typhimurium* in cylinders of agar when applying PEF treatments of 2.5 (5A and 5B) and 3.75 kV/cm (c and d) at 50 Hz in positions P2 (a and c) and 4 (b and d). \log_{10} cycles of actual inactivation (●) of *Salmonella Typhimurium*.

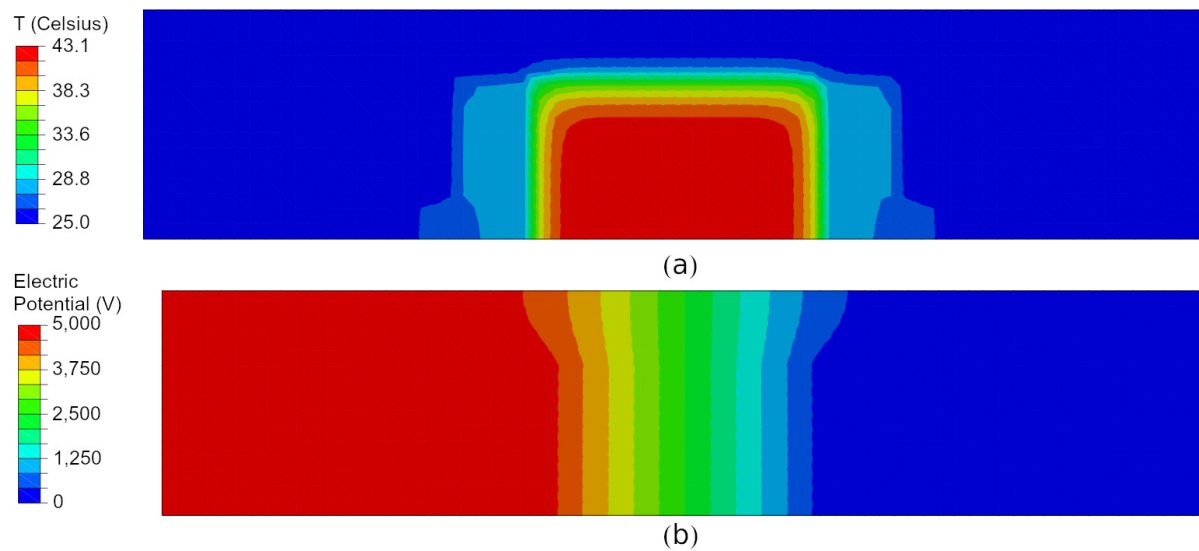


Figure 6: Finite element simulation of ohmic heating in the treatment chamber after a PEF treatment of 2.5 kV/cm at 50 Hz . (a) Temperature field. (b) Electric potential.

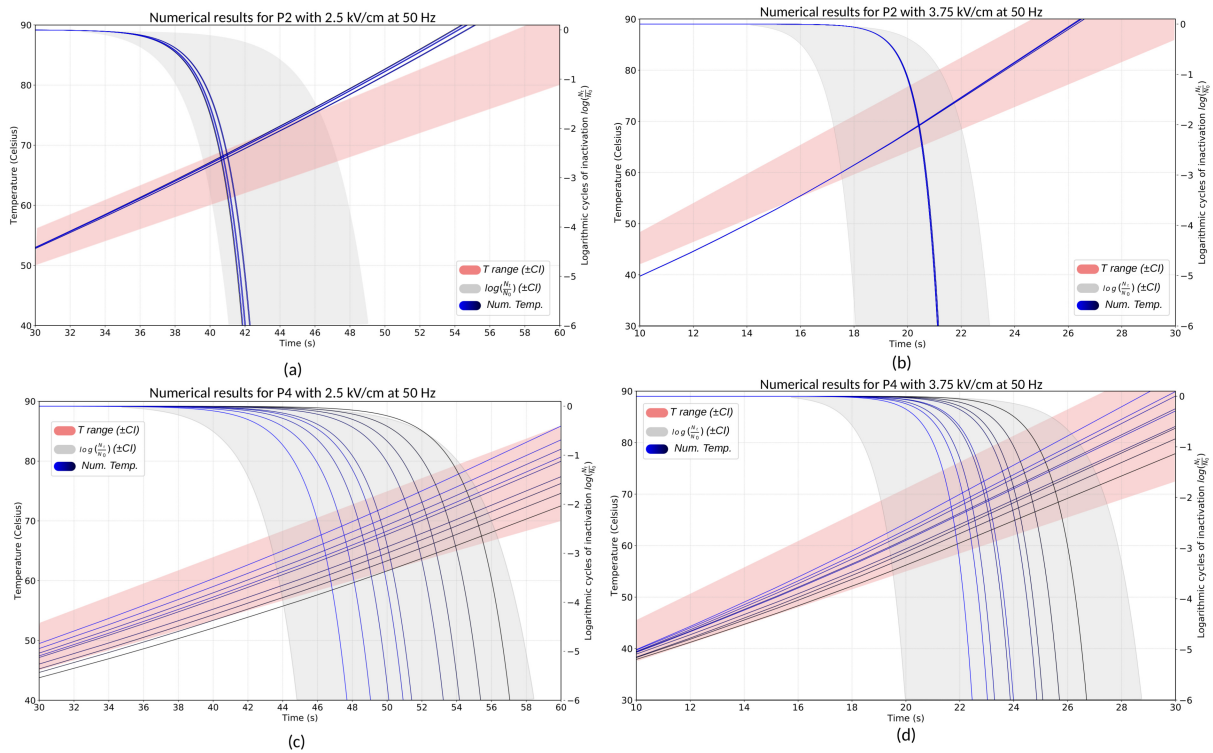


Figure 7: Simulated temperature and microbial inactivation (black-to-blue gradient lines) estimated by numerical simulation in positions P2 (a and c) and P4 (b and d) for simulations at 2.5 kV/cm and 50 Hz (a and b), and at 3.75 kV/cm and 50 Hz (c and d). Shaded areas represent the experimental ranges shown in Figure 5

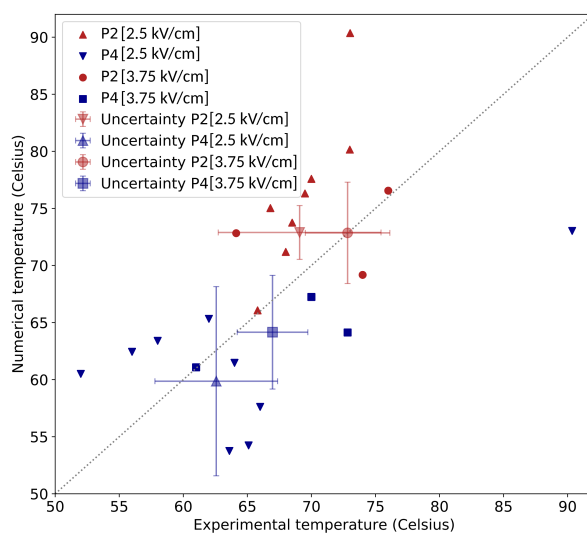


Figure 8: Correlation between experimental (x-axis) and simulated temperatures (y-axis). Triangles and inverted triangles represent measurements for experiments at 2.5 kV/cm and 50 Hz; circles and squares represent measurements for 3.75 kV/cm and 50 Hz, in red for position P2 (center) and in blue for position P4 (corner), respectively. Vertical error-bars represent uncertainty in experimental measurements, and horizontal error-bars represent uncertainty in numerical measurements (for experiments of different treatment time).